A SIMPLIFIED METHOD FOR PREDICTIONS OF SHAPE DISTORTIONS

Tonny Nyman[a], Magnus Svanberg[b] and Erik Hörberg[a]

[a]Saab Aerostructures, SE-581 88 Linköping, Sweden
[b]Swerea SICOMP AB, Box 271, 941 26 Piteå, Sweden
tonny.nyman@saabgroup.com

ABSTRACT

The use of composite material in primary structures is accelerating within the aircraft industry; actual examples are Boeing 787 (Dreamliner) and Airbus A350XWB. To design and manufacture a complex shaped composite article utilizing e.g. pre-preg is a demanding task. One challenge is to compensate tooling and lay-up and to control the process so that specified dimensional tolerances are met. Uncontrolled shape distortions in production cause delays and significant cost. Shape distortions of a complex geometry contain both local and global phenomena such as local spring-in, global spring-in, global twist, bending etc.

In this paper two different methodologies will be used for analysis of shape distortions and evaluated against experimental results. One method is very fast yet reasonably accurate if properly used. The other method implies modelling and simulation of how material properties and residual stresses evolve during the cure process [1,2,3,4,5]. The models used are, even though they are sufficiently accurate, sufficiently simplified to enable cost effective cure simulation also of larger structures. In a previous work [6] a typical C-spar was analysed using homogenizing properties assuming nominal fibre angles. In this work analysis is extended to include draping of the fibres that occur when a pre-preg is formed on to a double curved surface by using draping simulations. Also other important effects for shape distortions will be investigated i.e. stacking sequence and effect of cure scheme etc.

1. INTRODUCTION

In new aircraft programs like the Boeing 787 (Dreamliner) and Airbus A350XWB the composite content has increased to 50-60%. To be competitive in the future with the high demands on integration and short lead times there is an increased need for enhanced and harmonised data flow between disciplines in the design chain, such as assembly, tooling, production, measurements, geometry and stress office.

Due to the increased complexity of the structures tool compensation becomes more and more important. Today tool compensations are based on thumb rules in combination with production trials, which works very well for simple geometries. However, shape distortions of a complex geometry contain both local and global phenomena such as local spring-in, global spring-in, global twist, bending etc., illustrated in Figure 1.

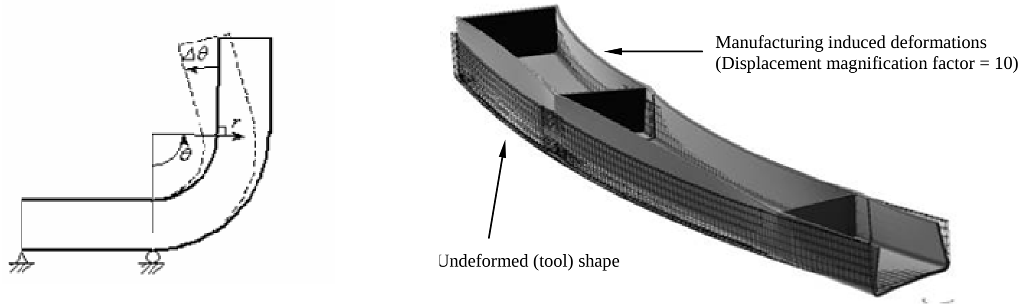

Figure 1. Local and global shape distortions. Geometry courtesy of BAESYSTEMS on behalf of the PRECIMOULD consortium.

With increased geometrical complexity of present and future composite articles the strategy based on rules of thumb in combinations with trials becomes very difficult, time consuming and expensive. For that reason tools for prediction of shape distortions are therefore an important step towards more efficient development of complex composite articles. In most high performance composites spring-in is the dominating and most important shape distortion, see the left figure in Figure 1. For a homogenous curved composite section subjected to a temperature difference the resulting spring-in, $\Delta\theta$ can be calculated [7] as,

$$\frac{\Delta\theta}{\theta} = (\alpha_\theta - \alpha_r) \cdot \Delta T \tag{1}$$

where ΔT, θ, α_θ and α_r are temperature difference, surrounding angle, in-plane and through thickness coefficient of thermal expansion, respectively.

Curing of a thermoset composite is a coupled thermal/structural problem. During cure a considerable amount of energy is released from the material and that has to be properly handled. Usually this is not a problem for thin structures with high fibre content cured under controlled conditions as in an autoclave.

In Ref. (6) a careful measurement, analyses and comparison of a typical C-spar was conducted. The objectives were to compare spring-in of the flanges, global behaviour as compared to an existing tool surface. The analysis was based on the articles nominal geometry. The results showed excellent agreement both regarding prediction of local spring-ins but also with respect to global behaviour. In this paper the same physical component will be used with the exception that the actual tool surface traditionally compensated for shape distortions will be used as a starting point and the effect of draping will be included by drape simulations.

2. METHODS OF ANALYSIS – MODELLING TECHNIQUES

In this paper two different methodologies for shape distortion analyses are described and used for analysis of a typical C-spar. One method is fairly simple and based on information from a process trial and a standard structural FE-analysis. The other method is a process simulation that does not require a process trial. A detailed description of the process simulation tool and the material model for a curing composite can be found in Refs. (-5).

2.1. Simplified methods

In-house methods used at Saab for predictions of shape distortions utilises a nonlinear elastic thermal stress analysis adjusted to information from process trials. This is the simplest and most common type of analysis of shape distortions. The advantage with this methodology is a relatively simple analysis, which requires only basic material data e.g. stiffness properties and coefficients of thermal expansion. Under right conditions this method is suitable for analysis of complex geometries, such as a C-spar of moderate thickness. The draw-back is that information from previous articles or a manufacturing trial is needed and that one parameter shall capture all possible mechanisms which make the analysis sensitive to changes, e.g. the analysis is only valid for the same cure conditions as in the manufacturing trials. The method is only valid for components without thermal gradients during cure e.g. thin components.

2.2. Cure simulation

Cure simulation is more general than the simplified approach and it is possible to analyse an article without data from previous process trial. The cure simulation also makes it possible to investigate the effect from different lay-ups, material or process conditions such as a modified cure schedule, which will be investigated further.

Curing of a composite is a complex thermal- chemical- mechanical process that involves shrinkage, thermal contraction and a dramatic change in the mechanical properties of the polymer. It has been shown that curing of a thermoset is viscoelastic and thermo rheologically complex. However, the viscoelastic behaviour during cure and in particular thermo rheologically complex behaviour is difficult to model accurately for a composite. This makes it attractive to simplify the behaviour and in a previous national research project by SAAB and Swerea SICOMP [-5] a material model that accounts for the relevant mechanisms during cure was developed. The advantage with the model is that it is possible to make a first assumption of shape distortions without manufacturing trials. The method picks up changes in the cure schedule, e.g. effects from cure temperature changes can be studied. It is possible to evaluate changes in lay-up and fibre volume fraction etc. without manufacturing trials. Some draw-backs are that the analysis becomes slightly more complex than an elastic thermal stress analysis and material properties that usually not are available e.g. chemical shrinkage and glass transition temperature as a function of degree of cure are required.

3. TYPICAL C-SPAR

As a benchmark for this paper an analysis of a typical C-spar is undertaken. The overall length of the spar is roughly 2 meters, a typical height and thickness of the conically shaped spar is 100mm and 6.5mm respectively. After manufacturing and trimming the C-spar was measured in a Metromec measuring machine. During the measurement the spar was aligned to a CAD model representing the tool surface so the total distortion after demoulding could be found, which is suitable for a quantitative comparison to predictions by FE-analysis. The gray lines in Figure 2 represent 8 sections starting with Section 1 in the right end of the spar. Each section consists of seven or eight measuring points, where two points were located at each flange.

Figure 2. Measurement arrangement for the C-spar.

4. ANALYSIS

Parameters to be investigated are influence of draping, i.e. altering of fibre angles, miss-oriented layers and different cure schemes. In particular two parameters will be monitored, spring-in of flanges and the global deformation of the spar, e.g. twist and lift.

The tool surface of the spar was meshed with ABAQUS S4R shell elements with well defined normal directions. The mesh was divided into six sections simulating production procedures and then each section was draped using COMPOSITE MODELLER for ABAQUS. The insertion point for each section was located at the inner flange and the propagation direction was from inner to outer flange. From the draped shell elements layered composite solid elements, with stacking sequence properties, were generated.
The deviation in fibre angles due to draping was roughly four degrees occurring at plies close to the ends of each draped sections. Analysis intended for cure simulation was handled separately in the general purpose FE-package ANSYS where the in-house material model for a curing thermoset was implemented using user defined subroutines.
A careful modelling of radii is necessary since the radii to a high degree rule the behaviour. It has earlier in an in-house investigation [8] been shown that 4-5 elements around the radius are sufficient to capture correct deformation behaviour.
The final mesh consists of three dimensional 8-node solid elements (C3D8R in ABAQUS), the number of nodes were 13398 and 6464 elements with five elements around the radius. The element type is a layered solid composite element with three integration points per layer. The coordinate system of the model was aligned to the coordinate system used in the measurements. With the spar web facing down, flanges pointing upwards, the x-axis was running along the web, y-axis in the height direction of the web and z-axis through the thickness of the web.

4.1. Material properties, boundary and initial conditions

To prevent rigid body motion the spar was supported at three points, two in the front and one in the back end marked with red circles in Figure 3. The lower left node (BC1), lower right node (BC2) and the upper node (BC3) were constrained in all directions, the z direction and in the y and z direction, respectively.
In order to compare the predicted to measured shape distortions the predicted results have to be aligned to the measured results, which was done by introducing a rigid body motion by a translation of the constrained nodes, [6].
The lamina properties presented in Table 1, valid at RT, have been used in the analysis of the C-spar. The lay-up both for the web and for the flanges was approximately 30/40/30% in the 0°/45°/90° direction.

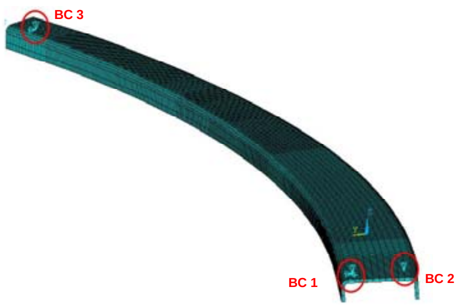

Figure 3. FE-mesh with boundary condition.

Table 1 Ply properties.

Material Type	Carbon pre-preg
E_l(GPa)	145
E_t(GPa)	8
G_{lt}(GPa)	4
ν (–)	0.3
Thickness (mm)	0.20
CTE_l	4e-8
CTE_t	4e-5

4.2. Simplified method

In the simplified analysis a temperature change representing the cooling of the component from the cure temperature to room temperature was used to create the shape distortions. When just the temperature is accounted for the shape distortion is

under estimated because many important factors are neglected e.g. the chemical shrinkage of the polymer. For that reason the coefficient of thermal expansion through the thickness have been replaced by a coefficient of process expansion, *CPE*.
In order to find a proper value of *CPE* results from a process trial or other components are needed. In this particular case a process trial has revealed that a *CPE* value of 1.6 times CTE_t is expected for this particular pre-preg system.

4.3. Cure simulation

The cure simulation requires more input for instance to keep track of the material state i.e. the relationship between T_g (Glass transition temperatures) and X (degree of cure) have to be known. At temperatures above T_g the polymer is soft, which is called the rubbery state and at temperatures below T_g the material is in glassy state. A common description of the relationship between is T_g and X is the DiBenedetto equation,

$$\frac{T_g - T_{g0}}{T_{g\infty} - T_{g0}} = \frac{\lambda \cdot X}{1-(1-\lambda)\cdot X} \qquad (2)$$

T_{g0}, $T_{g\infty}$ and λ is the glass transition temperature prior to cure, the glass transition temperature of the fully cured system (X = 1) and a material constant, respectively. Other important properties are the volumetric chemical shrinkage, which is around 5-7% for high temperature epoxy systems, a detailed description of required material properties and of the behaviour of a curing polymer can be found in [-5].
The required properties are unfortunately not known for this particular pre-preg system used in this case. However, it is possible to make a reasonable estimate from the properties of the well known RTM6 resin [9,10,11], which is a similar 180°C epoxy system, see Table 2. The fibres will not change during cure and only the stiffness properties and coefficient of thermal expansion is required, the properties used in this paper were found in a standard composite textbook [12]. From the properties of the resin and fibres the properties of the laminate in glassy state and in the rubbery state were estimated by self-consistent field micro mechanics [13] and three-dimensional laminate theory [14]. A fibre volume fraction of 60% was assumed, which together with the lay-up resulted in the laminate properties presented in Table 3 and the coefficient of thermal shrinkage and chemical shrinkage in Table 4.

Table 2 Properties for cure simulation of HexFlow® RTM6 resin.

Description	Property	Value	Unit	Source
T_g at X = 0, Eqn. (2)	T_{g0}	-11	°C	[11]
T_g at X = 1, Eqn. (2)	$T_{g\infty}$	206	°C	[11]
Constant in Eqn. (2)	λ	0.435	-	[11]
X at gelation	X_{gel}	0.59	Xgel (-)	[11]
Vol. chemical shrinkage	$\Delta V/V$	5.4	(%)	[10]

Table 3 Estimated engineering constants based on RTM6/carbon fibres.

	E_1 (GPa)	**E_2 (GPa)**	**E_3 (GPa)**	**ν_{12} (-)**	**ν_{13} (-)**	**ν_{23} (-)**	**G_{12} (GPa)**	**G_{23} (GPa)**	**G_{23} (GPa)**
Glassy	61.3	53.1	9.4	0.27	0.31	0.30	16.5	3.1	3.1
Rubbery	56.1	47.5	3.6	0.27	0.63	0.57	13.8	0.04	0.04

Table 4. Estimated expansion properties.

	Linear Thermal Expansion			Linear Chemical Shrinkage		
	CTE_1	CTE_2	CTE_3	LCS_1	LCS_2	LCS_3
Glassy	$2.6 \cdot 10^{-6}$	$3.5 \cdot 10^{-6}$	$6.0 \cdot 10^{-5}$	$-6.6 \cdot 10^{-4}$	$-8.5 \cdot 10^{-4}$	$-1.3 \cdot 10^{-2}$
Rubbery	$-2.7 \cdot 10^{-7}$	$-2.2 \cdot 10^{-7}$	$1.8 \cdot 10^{-4}$	$-1.6 \cdot 10^{-5}$	$-2.1 \cdot 10^{-5}$	$-2.1 \cdot 10^{-2}$

In some cases a component is isothermally cured under well controlled conditions and the temperature and degree of cure is considered spatially uniform throughout the component. This condition implies that the important part of the temperature evolution is known from the cure schedule and the degree of cure after each cure step can be found from measurements. In this case the evolution of temperature and degree of cure was applied as boundary conditions in the structural analysis and the gelation where the polymer transforms from a liquid to a solid material is the starting point for the analysis. In the cure simulation the interaction from tooling was modelled by constraining all nodes in the model during in-mould cure. At demoulding all nodes were released and only rigid body motion was suppressed as previous described and shown boundary conditions. This implies that the time scale used in the cure simulation is fictitious and that the cure schedule can be divided into following five calculation steps; 1. Cure shrinkage in rubbery state at 180°C, 2. Transition from rubbery to glassy state (vitrification), 3. Cure shrinkage in glassy state, 4. Cooling from the cure temperature to room temperature and finally 5. Demoulding, where the boundary conditions are changed, the residual stresses are released and the shape distortions are formed. In this case the final degree of cure is unknown but a reasonable estimate can be found based on experience with RTM6 [9].

5. RESULTS

5.1. Global – local effects

From the analysis global effects and more localized phenomena can be deduced. In general global effects show a typical lift upwards on the middle of the spar and a global twist, see Figure 4. The effect of draping, simulating production procedures, had no significant influence on global and local behaviour as compared to nominal fibre angles used in a previous investigation, [6]. The figure shows a contour plot of the shape distortions in the local z-direction, (same as the global x-direction).

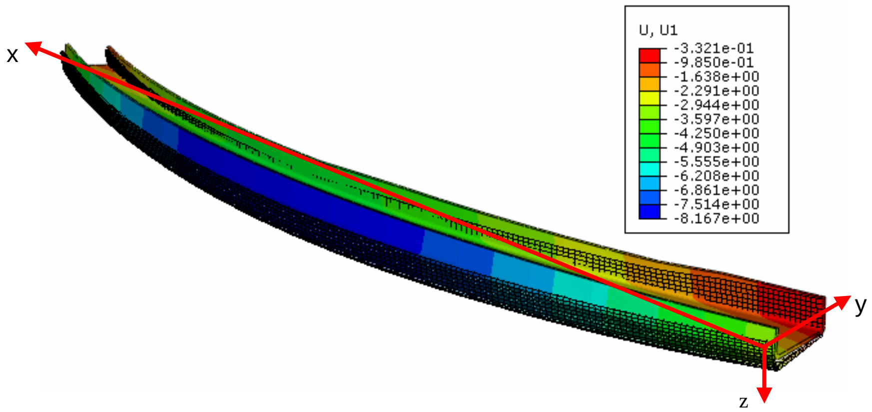

Figure 4. Contour plot of the predicted distortion in the z-direction, magnification = 5.

If one layer is misplaced, one of the 45 degree plies located close to inner mould line (IML) was changed to a minus 45 degree, a substantial change of lift could be observed. In comparison with a nominal sequence the lift was downwards and the twist was in the opposite direction, while spring-in angled was not effected, see Figure 5.

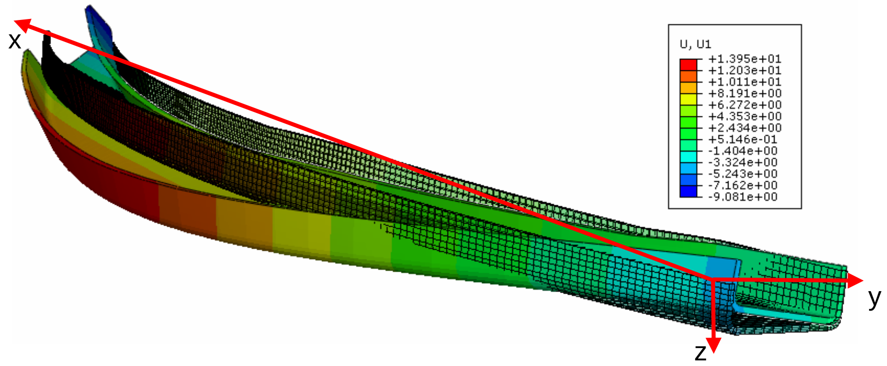

Figure 5. Displacement z missplaced layer, magnification = 5.

5.2. Comparison between measured and predicted distortion

A comparison of the distortion of the web between the FE-analysis and the experiments can be seen in Figure 6. The comparison covers the lift both for the nominal and the miss-oriented layer in two tracks. One track is close to the inner flange and the other adjacent to the outer flange. A good agreement between the measured and predicted distortion of the web can be seen for the nominal lay-up sequence. As seen in Figure 6 a miss-oriented layer drastically changes the deformation.

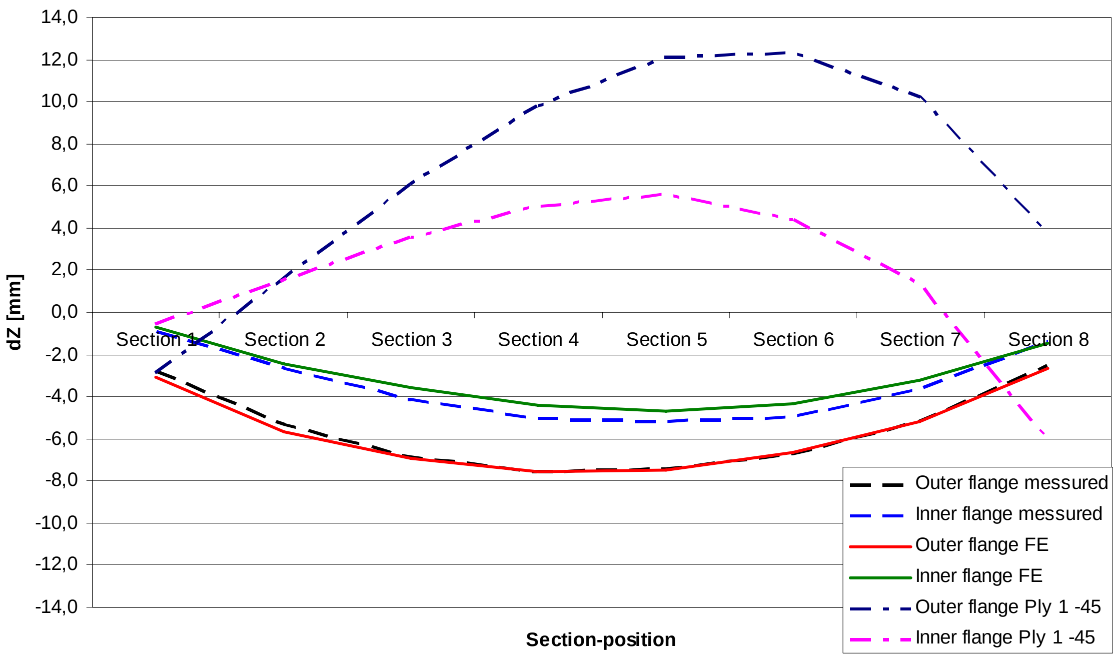

Figure 6. Comparison between predicted and measured distortion of the web.

In order to find the spring-in at each section a vector was constructed from the coordinates of two measured point respectively two nodes in the FE-model on each flange and web. Then the angle between the vectors was calculated, which represent the angle between the flange and web. The spring-in is the difference between this angle before and after the distortion and is presented for each section in Table 5.

Table 5 Comparison of calculated and measured spring-in angles

Outer flange	Spring-in [◦]	
Section	Measured	FE-model
1	1.24	1.17
2	1.15	1.04
3	1.08	1.01
4	1.13	1.07
5	1.14	1.04
6	1.08	1.09
7	1.16	1.14
8	1.12	1.19
Average	1.14	1.09

Inner flange	Spring-in [◦]	
Section	Measured	FE-model
1	1.05	1.00
2	1.15	1.10
3	1.12	1.09
4	1.13	1.07
5	1.08	1.11
6	1.08	1.15
7	1.07	1.09
8	1.11	1.10
Average	1.10	1.09

The analysis shows a spring-in of 1.09° for both the inner and outer flange and the average measured value is 1.14° and 1.10°, for the outer and inner flange, respectively. The measurements also show a variation of the spring-in angles for the different sections both for the inner and outer flange. The deviation between the average measured value and the predicted spring-in of the outer flange is 0.05° while for the inner flange the difference is 0.01°. A typical angle tolerance would be 0.4° compared to a maximum error of 0.1° which is a very good result.

5.3. Cure simulation

The degree of cure for different cure schedule can be found in the product data sheet [9], see Table 6. For a 180°C cure schedule the estimated spring-in by cure simulations is 1.0°, both for inner and outer flange. This value is slightly lower than the value by the simplified method. However, the value was obtained from the fundamental behavior of a curing thermoset and is not fitted to an experimental result. A common tolerance for 180°C curing is +15/-5°C, in Table 6 the corresponding degree of cure at 175 and 195°C have been estimated from information in the product data sheet of RTM6 [9]. With this information we can rerun the cure simulation and find out how the temperature tolerance effects the shape distortion. The result is presented in Table 6, which shows that the shape distortion is rather insensitive for cure temperature in the interval 180°C +15/-5°C.
At this point we have only considered one step cure schedule but in some cases it might be interested to use a two step cure schedule. By using cure simulation it is possible to estimate how this will affect the shape distortions. For that reason we consider a 120°C dwell temperature which results in a degree of cure of 81% according to Table 6 followed by a heating and final curing at 180°C (96%) before cooling and demoulding at room temperature. By including this information in the cure simulation the resulting estimated shape distortion is 0.73°, which is considerable less than the 1.00° obtained after a single step 180°C cure schedule. The same boundary conditions as before was used after demoulding but the translation to compare the calculated result to measured results was omitted to only show distortions. In Figure 7 the distortions of the web in z-direction have been plotted close to the inner and outer flanges, respectively. The blue lines shows the estimated distortion of the web after a one step cure schedule and the red lines shows the corresponding distortion after a two step cure schedule.

The conclusions from the cure simulations are that the shape distortions of the C-spar are not sensitive to small variation of cure temperature but a two step cure schedule can significantly reduce the shape distortions.

Table 6 Degree of cure of RTM6 resin.

Cure schedule	Degree of cure	Source	Spring-in estimated by cure simulation
160°C / 2h	0.91	[13]	-
180°C / 2h	0.96	[13]	1.03°
195°C	1.0	Extrapolation	1.13°
175°C	0.95	Interpolation	1.00°
120°C	0.81	Extrapolation	-

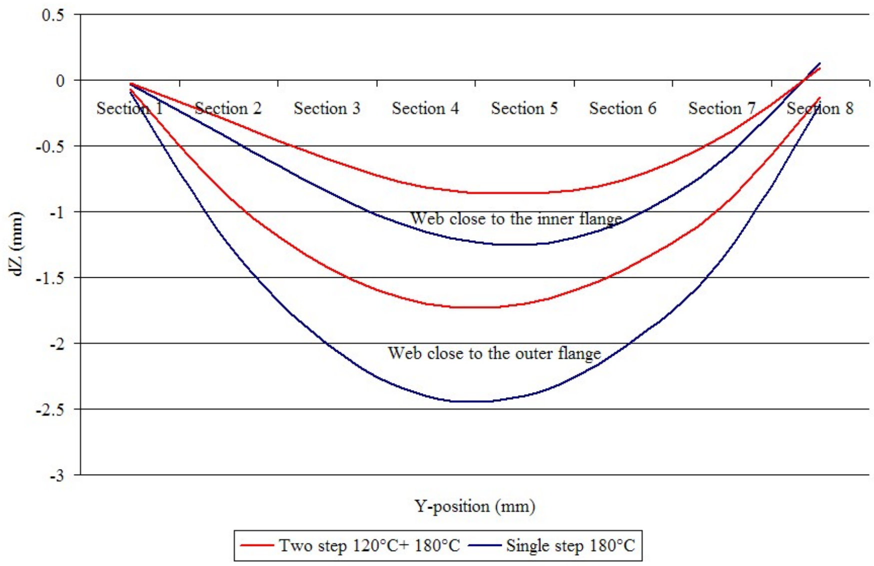

Figure 7. Distortion of the web estimated by cure simulation for a single step and two step cure schedule.

6. SUMMARY AND CONCLUSIONS

In general a good correspondence is achieved when predicting the deformation for a typical C-spar regarding global twist and deflection of the web and local spring-in of the flanges.

A substantial change in global behaviour was found when one layer is miss-placed. A 45 degree ply close to IML was interchanged to a -45 degree ply and the global lift was almost doubled.

The predicted spring-in angles of the outer and inner flange are slightly underestimated but the result is very good.

For current application, regarding thickness of article and plies, the influence of draping was negligible. For other thicknesses, draping orders and configurations this must be further investigated.

The importance of cure simulation has been high-lighted with respect to the possibility to see the effect of different cure schedules. For instance a two step cure schedule substantially reduces both lift and spring-in angles.

It should be emphasized that the prediction of a correct shape of a composite part could be extremely important when considering assembly tolerances, i.e. when several parts should be assembled with their own tolerances involved.

The cure simulation is more general than the simplified method and it is possible to analyse an article without data from previous process trial, which might be useful in some cases. The cure simulation also makes it possible to investigate the effect from changed lay-up, material or process conditions such a modified cure schedule etc. In order to do such investigations with the simplified method information from additional process trials are needed.

The methodology shown in this paper indicates that the number of tool iterations can be substantially reduced and consequently cost and time will be saved.

ACKNOWLEDGEMENTS

The work presented in this paper has been funded by the National Aviation Engineering Research Programme NFFP4-040 (KEKS) through VINNOVA (Swedish Governmental Agency for Innovation Systems)

We will acknowledge SIMULIA Scandinavia, for supplying us with the composite software COMPOSITE MODELLER and for valuable support.

REFERENCES

1. Svanberg JM, Holmberg JA. An experimental investigation on mechanisms for manufacturing induced shape distortion in homogenous balanced laminates. Composites Part A: Applied Science and Manufacturing 2001;32(6):827-838.
2. Svanberg JM. *Shape distortion of a non-isothermally cured composite angle bracket.* Plastics Rubbers and Composites 2002;31(9):398-404
3. Svanberg JM, Holmberg JA. *Prediction of shape distortions, Part I FE-implementation of a path dependent constitutive model.* Composites Part A: Applied Science and Manufacturing 2004;35(6):711-721.
4. Svanberg JM, Holmberg JA. *Prediction of shape distortions, Part II experimental validation and analysis of boundary conditions*. Composites Part A: Applied Science and Manufacturing 2004;35(6):723-734.
5. Svanberg JM, Altkvist C, Nyman T. *Prediction of shape distortions for a curved composite C-spar*. Journal of Reinforced Plastics and Composites. 2005;24(3):332-339.
6. Nyman T., Svanberg M. and Hörberg E. Cost Effective Shape Distortion Analysis of Composite Components. Presented at the Fibre Reinforced Composites Conference 2007 in Port Elizabeth, South Africa.
7. Radford DW, Diefendorf RJ. *Shape Instabilities in Composites Resulting from Laminate Anisotropy*. Journal of Reinforced Plastics and Composites 1993;12:58-75.
8. Skrinjar O. *Rear Spar mesh density test* ALCAS-31-00036-A01-WP124-LATERAL WING-REAR SPAR MESH DENSITY TEST.
9. Product Data Sheet: RTM 6. Hexcel Composites, Publication ITA 065a, September, 1998.
10. Holmberg JA. Resin Transfer Moulded Composite Materials. Doctoral Thesis, Luleå University of Technology, Department of Materials and Manufacturing Engineering, Division of Polymer Engineering, Report 1997:10, 1997.
11. Karkanas PI, Partridge IK. *Cure Modeling and Monitoring of Epoxy/Amine Resin System. II.*Network formation and Chemoviscosity Modeling. Journal of Applied Polymer Science 2000;77:2178-2188.
12. Hull D. An introduction to composite materials. Cambridge University Press, 1988.
13. Whitney JM, McCullough RL. *Micromechanical Material Modelling*, Delaware Composites Design Encyclopedia-Volume 2. 1990, 65-72, Technomic Pub. Co. Inc., Lancaster, Pennsylvania, USA.
14. Gudmundsson P, Zang W. An Analytic Model for Thermoelastic Properties of Composite Lamiantes Containing Transverse Matrix Cracks. International Journal of Solids and Structures 1993;30:3211-3231.